BİTLİS EREN ÜNİVERSİTESİ
FEN BİLİMLERİ DERGİSİ

ISSN: 2147-3129 / e-ISSN: 2147-3188

Article Type	: Research Article	**Year**	: 2025
Received	: June 4, 2025	**Volume**	: 14
Revised	: September 5, 2025	**Issue**	: 3
Accepted	: October 7, 2025	**Pages**	: 1759-1771
DOI	: 10.17798/bitlisfen.1714462		

EFFECT OF BUILD ORIENTATION AND HEAT TREATMENT ON SHEAR STRENGTH OF ADDITIVELY MANUFACTURED Ti6Al4V ALLOY

Gürkan KAYA [1], **Yusuf POLAT** [1, 2, *]

[1] *Erzurum Technical University, Mechanical Engineering Department, Erzurum, Türkiye*

[2] *Erzurum Technical University, High Technology Application and Research Center, Erzurum, Türkiye*

**** Corresponding Author:*** *yusuf.polat@erzurum.edu.tr*

ABSTRACT

This study investigates the effects of build orientation and heat treatment on the transverse shear properties of additively manufactured Ti6Al4V alloy produced by laser powder bed fusion (LPBF). Specimens were fabricated in three different build orientations (0°, 45°, and 90°) and subjected to heat treatment at 900 °C under argon gas atmosphere. Transverse shear strength was evaluated using the short beam shear test method. The results revealed that build orientation significantly affects both shear strength and ductility of materials. Compared to the 0° reference, the 45° and 90° samples showed an approximately 43% increase in shear strength, along with 56% and 103% increases in displacement, respectively. Heat treatment further enhanced the ductility, especially for the 45° oriented specimen, which exhibited the highest displacement and a 26% increase in shear strength compared with reference 0° sample. However, heat treatment slightly reduced the strength of the 45° and 90° specimens relative to their untreated counterparts. Fractographic analysis confirmed quasi-brittle failure with the presence of dimples, indicating enhanced ductility post-heat treatment. These findings provide novel insight into optimizing process parameters and post-processing strategies to improve the shear performance of LPBF Ti6Al4V components for critical structural applications.

Keywords: Laser powder bed fusion, Ti6Al4V alloy, Shear strength, Build orientation, Heat treatment, Fracture behavior.

1 INTRODUCTION

Additive manufacturing is an advanced manufacturing technology which is able to produce parts for high technology applications like biomedical [1], [2], [3], aerospace [4], [5],

and automotive [6], [7] in one step. The one step production technique is based on layer by layer construction of 3D designed models [8]. By these means, additive manufacturing allows the manufacturer to produce complex geometries with limited waste [9]. This unconventional and innovative manufacturing method is categorized to seven methods according to ASTM F2792-12 standard as powder bed fusion (PBF), sheet lamination, direct energy deposition, material extrusion, binder jetting, material jetting, and vat photopolymerization [10]. Among others, PBF is one of the most popular and utilized additive manufacturing technique [11], and it is most adaptable technique to produce 3D parts from various materials [12], [13].

Powder bed-based additive manufacturing by laser melting is of significance within the variety of other techniques [14]. The laser powder bed fusion (L-PBF) technology is based on melting powders which could be alloy or mixed powder by using laser source. This technique provides opportunities for production of various materials and components with almost near net geometry, flexibility in design, low production time [15], [16]. The CoCrFeMnNi alloy [17], CoCrMoW alloy [18], 316L stainless steel [19], Ti6Al4V alloy [16] are some common materials to be used for L-PBF method.

Ti6Al4V alloy is widely used in the aerospace and biomedical industries due to its advantageous properties, including a low coefficient of thermal expansion, biocompatibility, high strength-to-weight ratio, superior corrosion resistance, and greater strength compared to stainless steels [20]. As the most commonly used α+β titanium alloy, Ti6Al4V contains approximately 15% β phase, and its microstructure can be easily tailored through appropriate heat treatments. While the α phase is dominant at room temperature, the alloy transforms into a single β phase at around 995 °C [21]. Aluminum acts as an α-phase stabilizer enhancing strength, whereas vanadium stabilizes the β phase, improving ductility at room temperature and enabling a balanced combination of mechanical properties. The extra-low interstitial (ELI) grade of Ti6Al4V offers even higher fracture toughness and excellent damage tolerance, making it especially suitable for critical applications [22].

Several studies in the literature have emphasized that build orientation plays a crucial role in determining the anisotropic mechanical behavior of LPBF-fabricated Ti6Al4V components. Vrancken et al. [23] showed that anisotropy in LPBF-produced Ti6Al4V is strongly linked to build orientation and solidification behavior. Zhang et al. [24] further highlighted how tensile and shear properties vary significantly with orientation, with distinct fracture mechanisms observed across different build directions. More recently, Singh et al. [25] presented a comprehensive study demonstrating that build orientation directly affects tensile

strength, hardness, residual stress, and fracture mechanisms of Ti6Al4V alloys fabricated by L-PBF. Likewise, Yang et al. [26] systematically investigated multiple build orientations (0°, 30°, 45°, 60°, 90°) and reported orientation-dependent variations in microstructure and mechanical behavior, with the 45° samples showing the lowest tensile strength and ductility due to β-phase evolution and stair-step effects.

The heat-treated titanium alloy Ti6Al4V has been studied by researchers extensively. The studies were focused on effect of heat treatment on phase morphology [21], [27], kinetics model of heat treatment [28], [29], high temperature effect on alpha fraction [30], change in mechanical performance [31], [32], and so on. However, among other mechanical properties, there are no study on transverse shear strength of LPBF titanium alloy. The short beam shear method is suitable for the shear strength measurement of additively manufactured parts. Although L-PBF has many advantages for the production of complex parts to be used high tech applications, it also has drawbacks like poor ductility. The microstructure of parts produces by LPBF are affected by high cooling rate for highly dense part production requirements which yields poor ductility [23], [33].

Despite the extensive research on the tensile, compressive, and fatigue behavior of additively manufactured Ti6Al4V alloys, the transverse shear response of these materials has remained largely unexplored. Shear properties are critical for many load-bearing applications, where components are subjected to complex multiaxial stresses rather than uniaxial loading alone. In particular, the anisotropic nature of LPBF processed Ti6Al4V makes shear performance highly sensitive to build orientation and post-processing conditions, yet this aspect has not been systematically addressed in the literature. The present study bridges this knowledge gap by providing a comprehensive assessment of the shear strength and ductility of Ti6Al4V fabricated under different build orientations, with and without heat treatment.

2 MATERIALS AND METHODS

2.1 Materials

In this study, Ti6Al4V-ELI powder (General Electric, MA, USA), commercially available and produced via gas atomization, was utilized. Figure 1 presents the scanning electron microscope (SEM) image of the Ti6Al4V-ELI alloy powder used in this research. The powder particles were observed to have a predominantly spherical morphology, exhibit a uniform size distribution, and show no signs of agglomeration.

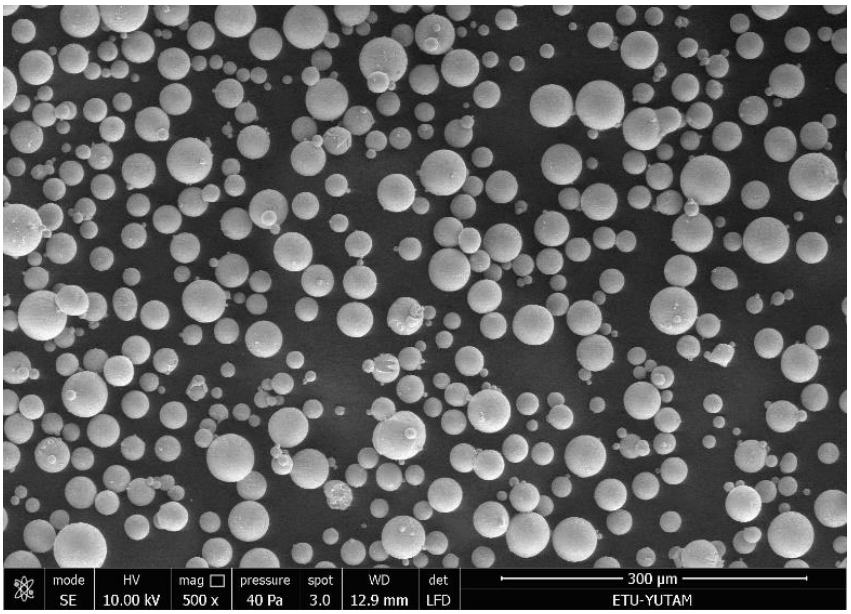


Figure 1. SEM image of Ti6Al4V-ELI powder.

2.2 Laser Powder Bed Fusion Technique

Additive manufacturing was carried out using a Concept Laser MLab-R LPBF system (max. 100 W), employing a bidirectional scanning strategy and operating in continuous laser mode. LPBF production process parameters was given in Table 1. To prevent oxidation, the entire fabrication process took place within an Argon (Ar) gas-shielded atmosphere. The specimens with 5 x 12 x 35 mm prismatic dimensions were produced by L-PBF method for short beam shear testing. Three different orientation angles (0°, 45° and 90°) were used during LPBF production. The schematic view of the samples on the build platform and post-production images are shown in Figure 2.

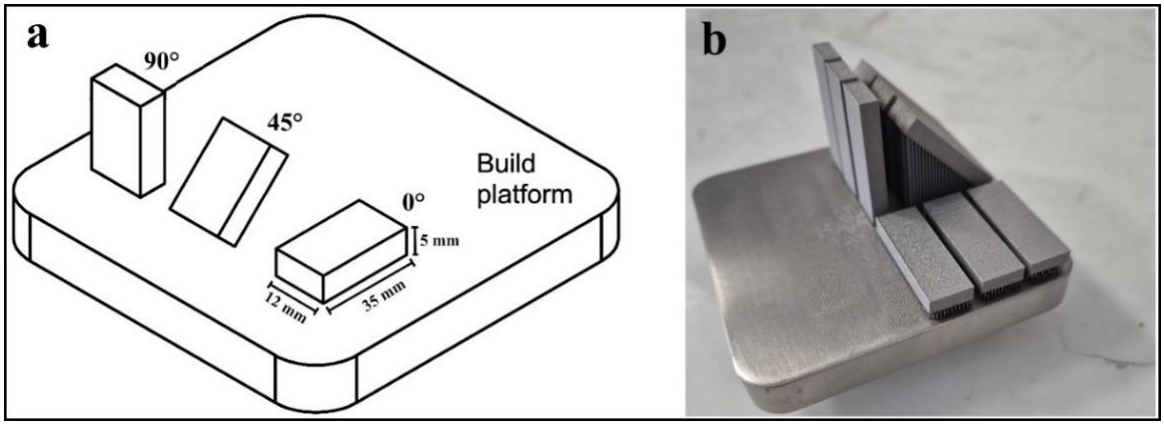


Figure 2. (a) Schematic view and (b) produced samples on the build platform.

Table 1. LPBF production parameters [16].

LPBF Process Parameters	Values
Laser power	80 W
Scanning speed	1125 mm/s
Layer thickness	25 µm
Hatch distance	45 µm

2.3 Heat Treatment

Samples fabricated using the LPBF technique were subjected to heat treatment. To minimize oxidation caused by exposure to the surrounding atmosphere, experiments were conducted in an Argon gas-controlled environment. The heat treatment was performed at 900 °C (HT900), within the temperature range between Tα and the Tβ (β transus temperature of 995 °C) [34]. Heat treatment procedure was conducted in a Protherm Furnace brand, atmosphere-controlled heat treatment system.

2.4 Transverse Shear Strength Test

The transverse shear strength test was conducted by using a short beam with 27 mm span length, and 5 mm x 12 mm cross section as seen in Figure 3. A 3-point bending test apparatus were used with a 1 mm/min crosshead speed. The diameter for supporting pins was selected as 3 mm, and the diameter of pin for force application was selected as 6 mm. An Instron 5900 universal static test device was used to apply the force to materials. The experimental setup of the test system is shown in Figure 3.

The shear strength was calculated by using transverse shear formula as given in following equation;

$$\tau = \frac{V.Q}{I.t}$$

In which V is the shear force, Q is the $(\bar{y}'.A')$, where A' is the area of the top (or bottom) part of the cross section, above (or below) the section plane where thickness t is measured, and $\bar{y}'$ is the distance from the neutral axis to the centroid of A'. For rectangular cross section the formula becomes as follows;

$$\tau = 0.75\frac{P}{b.h}$$

where P is the maximum force, b is width, and h is the thickness.

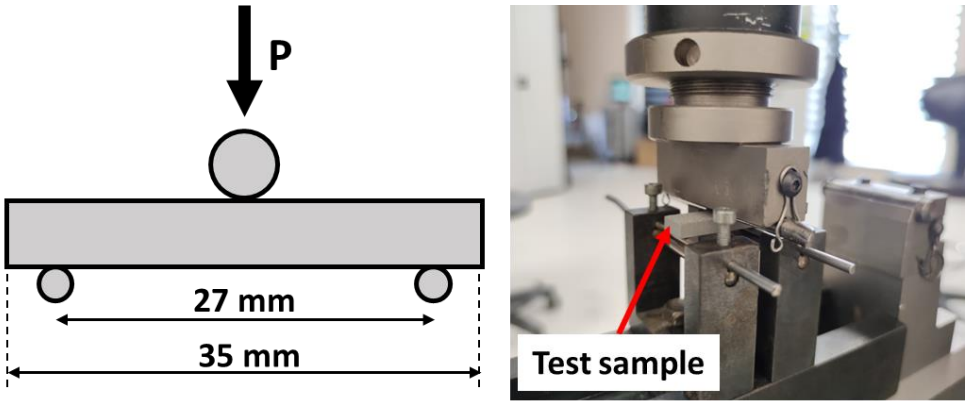


Figure 3. Schematic illustration for transverse shear test (left), and experimental setup (right).

3 RESULTS AND DISCUSSION

3.1 Post-process Analysis

The applied post-processing heat treatment at 900 °C (HT900), conducted between the α-transus and β-transus temperatures, had a clear influence on the microstructural evolution and mechanical performance of the LPBF-fabricated Ti6Al4V specimens. This treatment promoted the partial decomposition of the acicular α′ martensitic structure into an α+β lamellar morphology, which is consistent with previous reports [23], [31], [34]. As a result, the heat-treated samples generally exhibited improved ductility and defect tolerance, particularly evident in the 45° orientation, which showed the highest displacement (+36.2% compared to the as-built condition) and a 26% increase in shear strength relative to the 0° reference. Nevertheless, a slight reduction in ultimate strength was observed for the 45° and 90° orientations after heat treatment, which agrees with earlier studies indicating that lamellar α+β transformation enhances plasticity at the expense of strength [23], [32]. Fractography results further supported these findings, revealing a transition from quasi-brittle fracture surfaces in the as-built state to more ductile dimpled morphologies after heat treatment. These observations confirm that the applied post-processing heat treatment is an essential factor in tailoring the balance between strength and ductility in LPBF-produced Ti6Al4V components.

3.2 Transverse Shear Strength Test Results

The shear test was conducted to both untreated and heat-treated samples. The effect of build orientation and heat treatment were discussed. Simonelli et al. [35] investigated the influence of build orientation on the mechanical behavior of Ti6Al4V alloy fabricated by SLM,

demonstrating that the alignment of prior β grain boundaries relative to the applied axial load governed both the fracture mechanism and crack propagation. Figure 4 shows the shear stress – displacement curves for reference (0° build orientation), 45°, and 90° oriented samples during production. The results showed that the transverse shear strength for 45° and 90° samples are increased to nearly same values which is nearly 210 MPa. The displacement at maximum load is 1.463 mm for reference sample. The displacement of samples was increased with build orientation around 2.281 mm for 45°, while it is 2.964 mm for 90°. Table 2 summarized the force, displacement, and shear stress values of all samples, and it compares the improvements of heat-treatment for each orientation. The build orientation effect enhanced the shear strength nearly 43% for both angles. However, the improvement in displacement is different for 45° and 90° build orientations, which are 56% and 103%, respectively. The influence of build orientation on tensile and shear behavior is highly complex, as the mechanical response of additively manufactured materials is strongly governed by their microstructure and the distribution of internal defects [36]. In the case of Ti6Al4V fabricated in the horizontal direction, the content of fine needle-like α′ martensite is increased due to the elevated cooling rate during the selective laser melting process [37]. Moreover, the dimples observed in the horizontal specimen appear slightly larger and shallower compared to those in the vertical specimen, suggesting reduced ductility in the horizontally built sample [24].

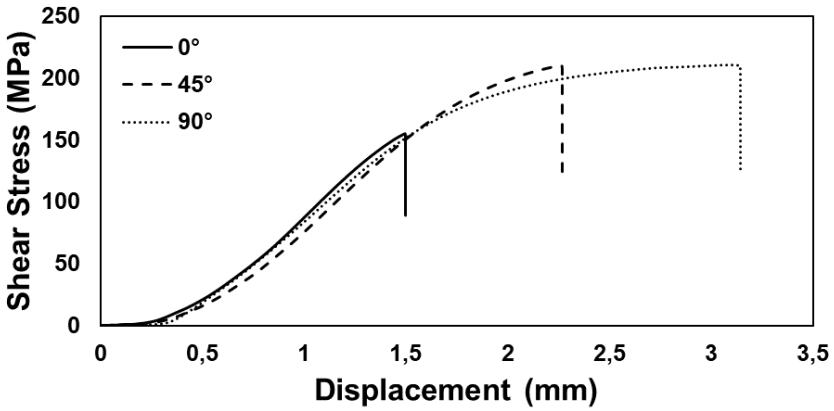


Figure 4. Shear stress – Displacement curves for untreated Ti6Al4V alloys.

The results in Figure 4 showed that the 90° build orientation enhanced the ductility of material more than 45°. In addition to build orientation, heat-treatment was applied to Ti6Al4V alloys to enhance their ductility. The effect of temperature improved the both shear strength and displacement of reference sample by nearly 15% and 48%, respectively. After heat-treatment, the displacement of 45° sample (HT_45°) increased to 3.108 mm (36.2% more than untreated sample, and maximum obtained) from 2.281 mm. However, the heat treatment did not change the displacement of 90° sample significantly.

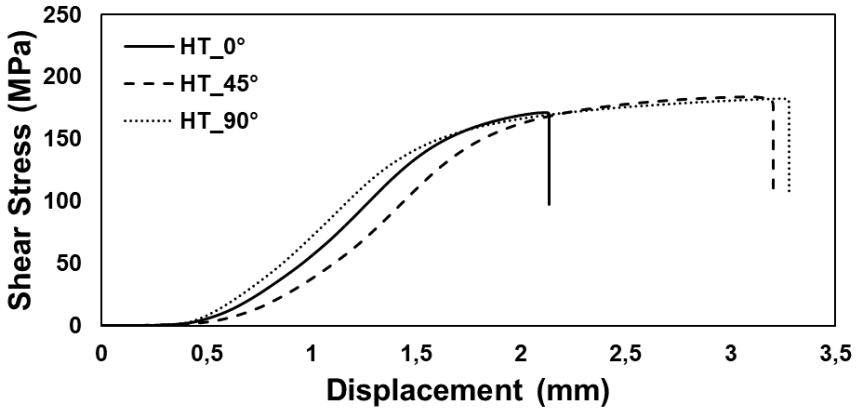


Figure 5. Shear stress – Displacement curves for heat-treated Ti6Al4V alloys.

The Figure 5 shows the Shear stress – displacement curve for heat-treated samples. The results showed that shear strength of reference sample is increased to 169 MPa, while it is decreased for oriented samples when compared with their oriented versions. The ratio of decrease is in shear strength nearly 12% for 45° orientated sample and 17% for 90° orientated sample. However, the strength values are higher than reference sample. Overall, the HT_45° sample with highest ductility and 26% increment in strength (compared with reference 0° sample) is the best sample for engineering applications. Sabban et al. [38] also found similar results that heat treatment is increasing the ductility of both vertically and horizontally build additively manufactured Ti6Al4V alloy. The lessening of defects like unmelted particles during production and porosity is expected to result in a further enhancement of ductility following heat treatment [38], [39].

Table 2. Force-Displacement-Shear strength values.

Sample code	Force (kN)	Displacement at max. force (mm)	Improvement in displacement (%)	Shear strength (MPa)	Improvement in shear strength (%)
0°	11.74±0.91	1.463±0.048	-	146.7±11.39	-
HT_0°	13.55±0.14	2.165±0.109	+47.9	169.4±1.69	+15.5
45°	16.81±0.04	2.281±0.032	-	210.2±0.47	-
HT_45°	14.81±0.12	3.108±0.065	+36.2	185.1±1.50	-11.9
90°	16.82±0.02	2.964±0.179	-	210.2±0.25	-
HT_90°	14.16±0.65	2.878±0.525	-2.9	176.9±8.10	-15.8

3.3 Fractography Analysis

SEM images of the fracture surfaces of untreated and heat-treated samples after the shear test are presented in Figure 6. The left column of the figure (Figure 6a-c) shows the fracture surfaces of untreated samples, and the right column (Figure 6d-f) shows the fracture

surfaces of heat-treated samples. In the horizontally build (0°) sample, the loading direction is perpendicular to the building direction, while in the vertically build (90°) sample, it is parallel to the building direction. In the sample produced at a 45° angle, the loading direction is at an angle to the building direction.

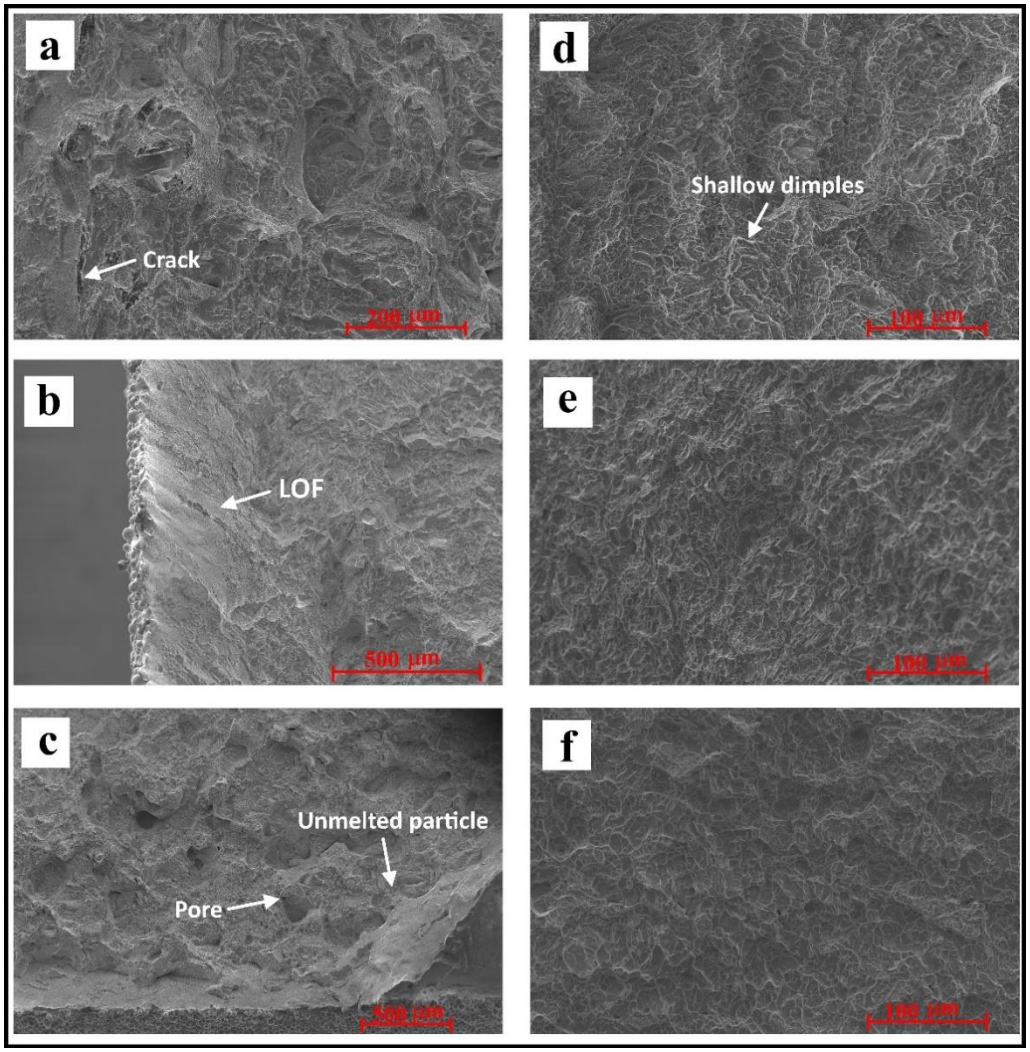


Figure 6. SEM images of fracture surfaces of shear samples, (a) 0°, (b) 45°, (c) 90°, (d) HT_0°, (e) HT_45° and (f) HT_90°.

Upon examination of the fracture surfaces of the specimens following shear tests, it was generally observed that the failure mode corresponded to a quasi-brittle fracture. Materials containing pores, lack of fusion (LOF), and microcracks due to the manufacturing process can exhibit such quasi-brittle behavior (Figure 6a-c). The defects are randomly distributed in the material. In this context, this type of fracture is expected in materials produced by LPBF. A shallow dimples structure, which is a typical indicator of ductile fracture, was observed across a large portion of the cross-sectional area (Figure 6d–f). The dimples observed in the vertically fabricated (90°) specimen are somewhat narrower and deeper compared to those in the

horizontally fabricated (0°) one, indicating that the vertical specimen has undergone more intense plastic deformation. Consequently, this indicates that the elongation at failure of the vertically build specimen is higher [24].

Due to the fracture characteristics of the samples under shear, the overall fracture morphology is relatively flat, and pit-free regions resulting from the friction of the fracture surfaces are observed in the edge regions (Figure 6b). In addition, it is seen that in the specimen build at a 45° angle, the LOF defect extends angularly along the shear loading direction, which is caused by the friction between the two fracture surfaces.

4 CONCLUSION

In this study, the influence of build orientation and post-process heat-treatment on the transverse shear properties of Ti6Al4V alloy fabricated via LPBF was systematically investigated. The main conclusions are as follows:

- Compared to the horizontally build (0°) samples, both 45° and 90° orientations enhanced the transverse shear strength by approximately 43%. The most significant improvement in ductility was observed in the 90° oriented sample with a 103% increase in displacement at maximum force.
- Post-process heat treatment at 900 °C under an inert atmosphere led to an increase in ductility across most build orientations. Notably, the HT_45° sample exhibited the highest displacement (3.108 mm), corresponding to a 112% improvement in ductility and a 26% increase in shear strength over the reference sample. However, heat treatment slightly reduced the strength of the 45° and 90° samples compared to their untreated counterparts.
- SEM analysis revealed a transition from quasi-brittle fracture surfaces in untreated samples to more ductile features (dimples) after heat treatment, confirming the improvement in ductility. The LOF defects and microstructural features induced by LPBF were responsible for the fracture behavior, which varied with orientation and heat treatment.
- HT_45° sample offers the most balanced mechanical performance, with improved strength and ductility, making it the most promising candidate for applications requiring resistance to shear loading.

Overall, this study provides a novel and comprehensive understanding of the shear performance of LPBF Ti6Al4V, emphasizing the critical role of build orientation and heat treatment. The outcomes can guide the development of optimized design and processing strategies for high-performance components in aerospace, biomedical, and structural applications.

Conflict of Interest Statement

There is no conflict of interest between the authors.

Statement of Research and Publication Ethics

The study is complied with research and publication ethics.

Artificial Intelligence (AI) Contribution Statement

This manuscript was entirely written, edited, analyzed, and prepared without the assistance of any artificial intelligence (AI) tools. All content, including text, data analysis, and figures, was solely generated by the authors.

Contributions of the Authors

G. Kaya and Y. Polat designed the conceptualization of the study, and contributed similar effort to writing of the manuscript. G. Kaya performed the production of test samples, and Y. Polat performed the shear strength tests. Discussion on the results were written by both authors.

REFERENCES

[1] G. Liu *et al.*, 'Development of Bioimplants with 2D, 3D, and 4D Additive Manufacturing Materials', *Engineering*, vol. 6, no. 11, pp. 1232–1243, Nov. 2020, doi: 10.1016/j.eng.2020.04.015.

[2] X. Wang *et al.*, 'Topological design and additive manufacturing of porous metals for bone scaffolds and orthopaedic implants: A review', *Biomaterials*, vol. 83, pp. 127–141, Mar. 2016, doi: 10.1016/j.biomaterials.2016.01.012.

[3] E. Alabort, D. Barba, and R. C. Reed, 'Design of metallic bone by additive manufacturing', *Scripta Materialia*, vol. 164, pp. 110–114, Apr. 2019, doi: 10.1016/j.scriptamat.2019.01.022.

[4] V. Madhavadas *et al.*, 'A review on metal additive manufacturing for intricately shaped aerospace components', *CIRP Journal of Manufacturing Science and Technology*, vol. 39, pp. 18–36, Nov. 2022, doi: 10.1016/j.cirpj.2022.07.005.

[5] V. Mohanavel, K. S. Ashraff Ali, K. Ranganathan, J. Allen Jeffrey, M. M. Ravikumar, and S. Rajkumar, 'The roles and applications of additive manufacturing in the aerospace and automobile sector', *Materials Today: Proceedings*, vol. 47, pp. 405–409, Jan. 2021, doi: 10.1016/j.matpr.2021.04.596.

[6] V. Juechter, M. M. Franke, T. Merenda, A. Stich, C. Körner, and R. F. Singer, 'Additive manufacturing of Ti-45Al-4Nb-C by selective electron beam melting for automotive applications', *Additive Manufacturing*, vol. 22, pp. 118–126, Aug. 2018, doi: 10.1016/j.addma.2018.05.008.

[7] M. S. Muhammad, L. Kerbache, and A. Elomri, 'Potential of additive manufacturing for upstream automotive supply chains', *Supply Chain Forum: An International Journal*, vol. 23, no. 1, pp. 1–19, Jan. 2022, doi: 10.1080/16258312.2021.1973872.

[8] F. A. Talebi *et al.*, 'Spreadability of powders for additive manufacturing: A critical review of metrics and characterisation methods', *Particuology*, vol. 93, pp. 211–234, Oct. 2024, doi: 10.1016/j.partic.2024.06.013.

[9] L. Jin *et al.*, 'Big data, machine learning, and digital twin assisted additive manufacturing: A review', *Materials & Design*, vol. 244, p. 113086, Aug. 2024, doi: 10.1016/j.matdes.2024.113086.

[10] I. Astm, 'ASTM F2792-10: standard terminology for additive manufacturing technologies', *ASTM International*, 2010.

[11] D. Sarkar, A. Kapil, and A. Sharma, 'Advances in computational modeling for laser powder bed fusion additive manufacturing: A comprehensive review of finite element techniques and strategies', *Additive Manufacturing*, vol. 85, p. 104157, Apr. 2024, doi: 10.1016/j.addma.2024.104157.

[12] T. DebRoy *et al.*, 'Additive manufacturing of metallic components – Process, structure and properties', *Progress in Materials Science*, vol. 92, pp. 112–224, Mar. 2018, doi: 10.1016/j.pmatsci.2017.10.001.

[13] S. Chowdhury *et al.*, 'Laser powder bed fusion: a state-of-the-art review of the technology, materials, properties & defects, and numerical modelling', *Journal of Materials Research and Technology*, vol. 20, pp. 2109–2172, 2022.

[14] J.-P. Kruth, G. Levy, F. Klocke, and T. H. C. Childs, 'Consolidation phenomena in laser and powder-bed based layered manufacturing', *CIRP Annals*, vol. 56, no. 2, pp. 730–759, Jan. 2007, doi: 10.1016/j.cirp.2007.10.004.

[15] W. Abd-Elaziem *et al.*, 'On the current research progress of metallic materials fabricated by laser powder bed fusion process: a review', *Journal of Materials Research and Technology*, vol. 20, pp. 681–707, Sept. 2022, doi: 10.1016/j.jmrt.2022.07.085.

[16] G. Kaya *et al.*, 'Effects of process parameters on selective laser melting of Ti6Al4V-ELI alloy and parameter optimization via response surface method', *Materials Science and Engineering: A*, vol. 885, p. 145581, Oct. 2023, doi: 10.1016/j.msea.2023.145581.

[17] C. Bulut, F. Yıldız, T. Varol, G. Kaya, and T. O. Ergüder, 'Effects of Selective Laser Melting Process Parameters on Structural, Mechanical, Tribological and Corrosion Properties of CoCrFeMnNi High Entropy Alloy', *Met. Mater. Int.*, vol. 30, no. 11, pp. 2982–3004, Nov. 2024, doi: 10.1007/s12540-024-01694-w.

[18] T. Varol, H. C. Aksa, F. Yıldız, S. B. Akçay, G. Kaya, and M. Beder, 'Influence of post processing on the mechanical properties and wear behavior of selective laser melted Co-Cr-Mo-W alloys', *Tribology International*, vol. 192, p. 109336, Apr. 2024, doi: 10.1016/j.triboint.2024.109336.

[19] G. Kaya, U. Köklü, T. O. Ergüder, F. Cengiz, and F. Yıldız, 'Effects of build orientation and hatch spacing on high-speed milling behavior of L-PBF 316L stainless steel', *Materials Testing*, vol. 65, no. 10, pp. 1571–1581, Oct. 2023, doi: 10.1515/mt-2023-0210.

[20] J. Zhao, H. Liu, Y. Zhou, Y. Chen, and J. Gong, 'Effect of relative density on the compressive properties of Ti6Al4V diamond lattice structures with shells', *Mechanics of Advanced Materials and Structures*, vol. 29, no. 22, pp. 3301–3315, Aug. 2022, doi: 10.1080/15376494.2021.1893418.

[21] T. Ahmed and H. J. Rack, 'Phase transformations during cooling in α + β titanium alloys', *Materials Science and Engineering: A*, vol. 243, no. 1–2, pp. 206–211, 1998, doi: 10.1016/s0921-5093(97)00802-2.

[22] A. A. Antonysamy, *Microstructure, texture and mechanical property evolution during additive manufacturing of Ti6Al4V alloy for aerospace applications*. The University of Manchester (United Kingdom), 2012. Accessed: May 02, 2025. [Online]. Available: https://search.proquest.com/openview/6d22965546ce3092918e9ad2280b68fc/1?pq-origsite=gscholar&cbl=51922

[23] B. Vrancken, L. Thijs, J.-P. Kruth, and J. Van Humbeeck, 'Heat treatment of Ti6Al4V produced by Selective Laser Melting: Microstructure and mechanical properties', *Journal of Alloys and Compounds*, vol. 541, pp. 177–185, Nov. 2012, doi: 10.1016/j.jallcom.2012.07.022.

[24] H. Zhang, T. Gao, C. Xu, L. Zhao, H. Song, and G. Huang, 'Study on the Tensile and Shear Behaviors of Selective Laser Melting Manufactured Ti6Al4V', *Met. Mater. Int.*, vol. 29, no. 10, pp. 2852–2864, Oct. 2023, doi: 10.1007/s12540-023-01433-7.

[25] P. K. Singh, S. Kumar, P. K. Jain, and U. S. Dixit, 'Effect of Build Orientation on Metallurgical and Mechanical Properties of Additively Manufactured Ti-6Al-4V Alloy', *J. of Materi Eng and Perform*, vol. 33, no. 7, pp. 3476–3493, Apr. 2024, doi: 10.1007/s11665-023-08218-4.

[26] X. Yang *et al.*, 'Multi-build orientation effects on microstructural evolution and mechanical behavior of truly as-built selective laser melting Ti6Al4V alloys', *Journal of Materials Research and Technology*, vol. 30, pp. 3967–3976, May 2024, doi: 10.1016/j.jmrt.2024.04.031.

[27] I. Katzarov, S. Malinov, and W. Sha, 'Finite element modeling of the morphology of β to α phase transformation in Ti-6Al-4V alloy', *Metall Mater Trans A*, vol. 33, no. 4, pp. 1027–1040, Apr. 2002, doi: 10.1007/s11661-002-0204-4.

[28] N. Stefansson, S. L. Semiatin, and D. Eylon, 'The kinetics of static globularization of Ti-6Al-4V', *Metall Mater Trans A*, vol. 33, no. 11, pp. 3527–3534, Nov. 2002, doi: 10.1007/s11661-002-0340-x.

[29] S. Malinov, Z. Guo, W. Sha, and A. Wilson, 'Differential scanning calorimetry study and computer modeling of β ⇒ α phase transformation in a Ti-6Al-4V alloy', *Metall Mater Trans A*, vol. 32, no. 4, pp. 879–887, Apr. 2001, doi: 10.1007/s11661-001-0345-x.

[30] R. Pederson, O. Babushkin, F. Skystedt, and R. Warren, 'Use of high temperature X-ray diffractometry to study phase transitions and thermal expansion properties in Ti-6Al-4V', *Materials Science and Technology*, vol. 19, no. 11, pp. 1533–1538, 2003, doi: 10.1179/026708303225008013.

[31] M.-T. Tsai *et al.*, 'Heat-treatment effects on mechanical properties and microstructure evolution of Ti-6Al-4V alloy fabricated by laser powder bed fusion', *Journal of Alloys and Compounds*, vol. 816, p. 152615, Mar. 2020, doi: 10.1016/j.jallcom.2019.152615.

[32] S. A. Etesami, B. Fotovvati, and E. Asadi, 'Heat treatment of Ti-6Al-4V alloy manufactured by laser-based powder-bed fusion: Process, microstructures, and mechanical properties correlations', *Journal of Alloys and Compounds*, vol. 895, p. 162618, 2022.

[33] L. Thijs, F. Verhaeghe, T. Craeghs, J. V. Humbeeck, and J.-P. Kruth, 'A study of the microstructural evolution during selective laser melting of Ti–6Al–4V', *Acta Materialia*, vol. 58, no. 9, pp. 3303–3312, May 2010, doi: 10.1016/j.actamat.2010.02.004.

[34] X. Yan *et al.*, 'Effect of heat treatment on the phase transformation and mechanical properties of Ti6Al4V fabricated by selective laser melting', *Journal of Alloys and Compounds*, vol. 764, pp. 1056–1071, Oct. 2018, doi: 10.1016/j.jallcom.2018.06.076.

[35] M. Simonelli, Y. Y. Tse, and C. Tuck, 'Effect of the build orientation on the mechanical properties and fracture modes of SLM Ti–6Al–4V', *Materials Science and Engineering: A*, vol. 616, pp. 1–11, Oct. 2014, doi: 10.1016/j.msea.2014.07.086.

[36] J. M. Jeon *et al.*, 'Effects of microstructure and internal defects on mechanical anisotropy and asymmetry of selective laser-melted 316L austenitic stainless steel', *Materials Science and Engineering: A*, vol. 763, p. 138152, Aug. 2019, doi: 10.1016/j.msea.2019.138152.

[37] Z. Xie, Y. Dai, X. Ou, S. Ni, and M. Song, 'Effects of selective laser melting build orientations on the microstructure and tensile performance of Ti–6Al–4V alloy', *Materials Science and Engineering: A*, vol. 776, p. 139001, Mar. 2020, doi: 10.1016/j.msea.2020.139001.

[38] R. Sabban, S. Bahl, K. Chatterjee, and S. Suwas, 'Globularization using heat treatment in additively manufactured Ti-6Al-4V for high strength and toughness', *Acta Materialia*, vol. 162, pp. 239–254, Jan. 2019, doi: 10.1016/j.actamat.2018.09.064.

[39] C. Wang, Y. Lei, and C. Li, 'Achieving an Excellent Strength and Ductility Balance in Additive Manufactured Ti-6Al-4V Alloy through Multi-Step High-to-Low-Temperature Heat Treatment', *Materials*, vol. 16, no. 21, p. 6947, Jan. 2023, doi: 10.3390/ma16216947.